Electronic Supplementary Material (ESI) for Soft Matter.

Supplementary Information

A mathematical finance approach to the stochastic and intermittent viscosity fluctuations in living cells

Claude Bostoen* and Jean-François Berret*

Outline

Movie#1 – Sequence showing the internalization of magnetic wires in NIH/3T3 fibroblast cells.

Keywords: Active microrheology – Living cells – Cell biomechanics - Stochastic processes - Sub-diffusive mean-reverting process -
Corresponding authors:
c.bostoen@polymers.nl
jean-francois.berret@univ-paris-diderot.fr

Revised version sent to Soft Matter
Monday, May 18, 20

Supplementary Information S1 – Geometric characteristics of the wires used in this work

---

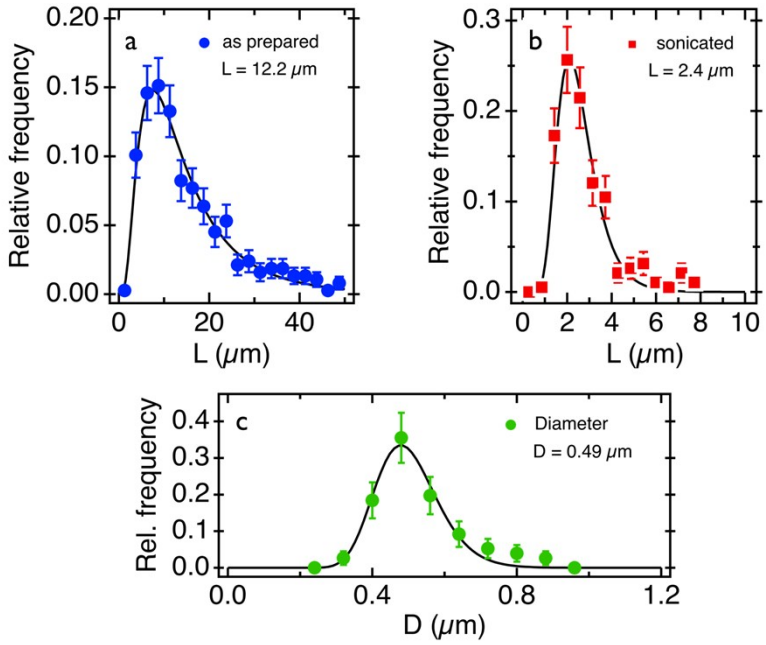

Figure S1: a, b) Size distribution of the wires prior and after sonication, respectively. Error bars are defined as the standard error of measurement (sem). **c)** Diameter distribution for the same wires.

Supplementary Information S2 – Spontaneous internalization of magnetic wires in fibroblasts

---

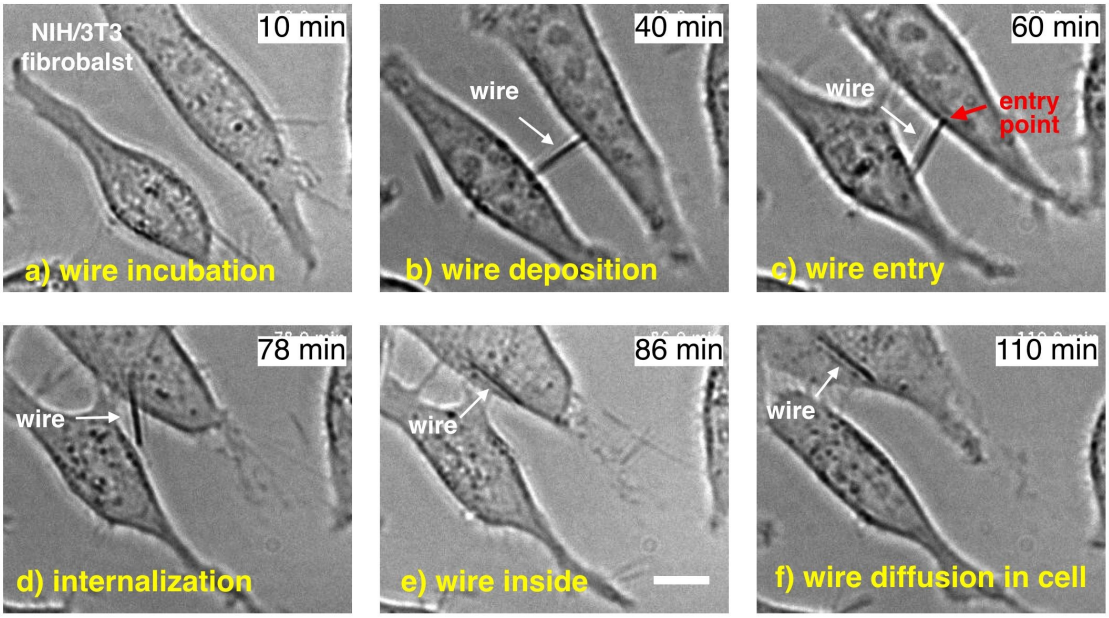

Figure S2: Snapshots of NIH/3T3 fibroblasts at different times after their incubation with magnetic wires. **a)** 10 min after the incubation, wires have not yet sedimented down to the cell layer. **b)** At 40 min a 6 µm wire in contact with two cells can be observed. **c)** The wire enters spontaneously inside the upper cell (rad arrow) 60 min after the incubation. **d)** The entry mechanism takes around 25 minutes. **e)** and **f)** the wire is in the cell and diffuses freely in the cytoplasm. The bar is 5 µm.

Supplementary Information S3 – Complementary data showing the critical frequency $\omega_C(t)$ and the shear viscosity $\eta(t)$ time series

---

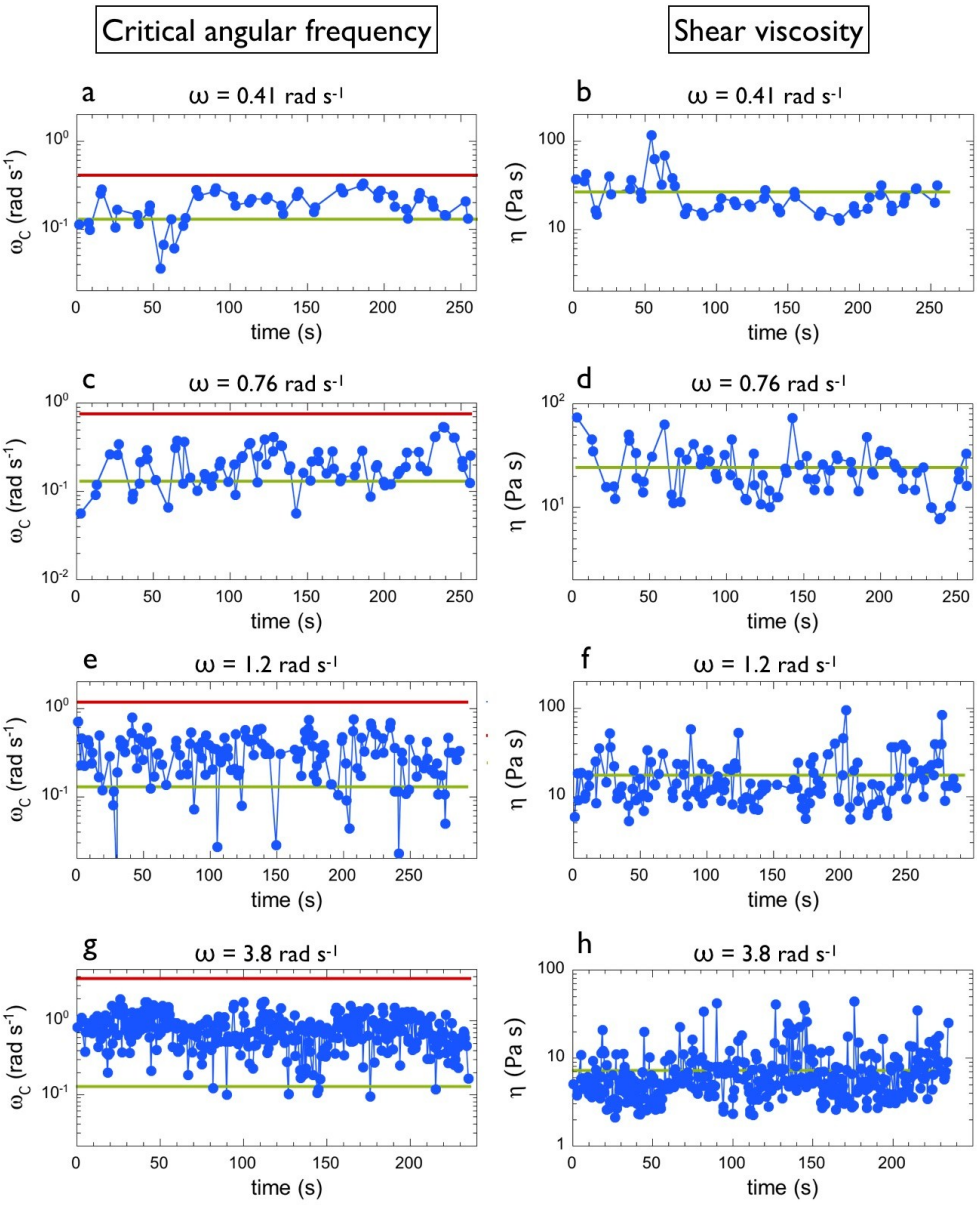

Figure S3: Time dependences of the critical frequency $\omega_C(t)$ (**a,c,e,g**) and of the shear viscosity $\eta(t)$ (**b,d,f,h**) obtained at the angular frequencies ω = 0.41, 0.76, 1.2 and 3.8 rad s^{-1}, as indicated. The horizontal lines in the $\omega_C(t)$-plots are the applied frequency (red) and the critical frequency determined in Fig. 2. The horizontal lines in green (right panels) show the viscosity averaged over time $\bar{\eta}(t)$. These data are complementary from those in Fig. 3 and again display large temporal fluctuations.

Supplementary Information S4 – Details on the method used to determine the time dependent viscosity and removal of outliers

---

The objective is here to transform a $\theta(t)$-time series determined from the wire rotation movies into 2 measurable quantities, the average rotation velocity $\Omega(t)$ and the oscillation amplitude $\theta_B(t)$. Each of these parameters are obtained at the time scale of a single oscillation in the non-synchronous regime ($\omega > \omega_C$).

As an illustration, we consider the time series obtained with a 2.8 µm wire rotating in a fibroblast cell at the frequency ω = 0.36 rad s^{-1} shown in Fig. S4. Over the time scale of 250 s, $\theta(t)$ exhibit three distinct regimes. Up to 140 s, the oscillations are steady and the overall signal is associated with an average rotation velocity of Ω_1 = 0.003 rad s^{-1}. The wire then accelerates between 140 s and 170 s at Ω_2 = 0.15 rad s^{-1}, that is half of the excitation frequency. Later, a third regime of steady oscillations eventually shows up until the experiment is stopped. This phenomenon is attributed to the change of the local viscosity $\eta(t)$.

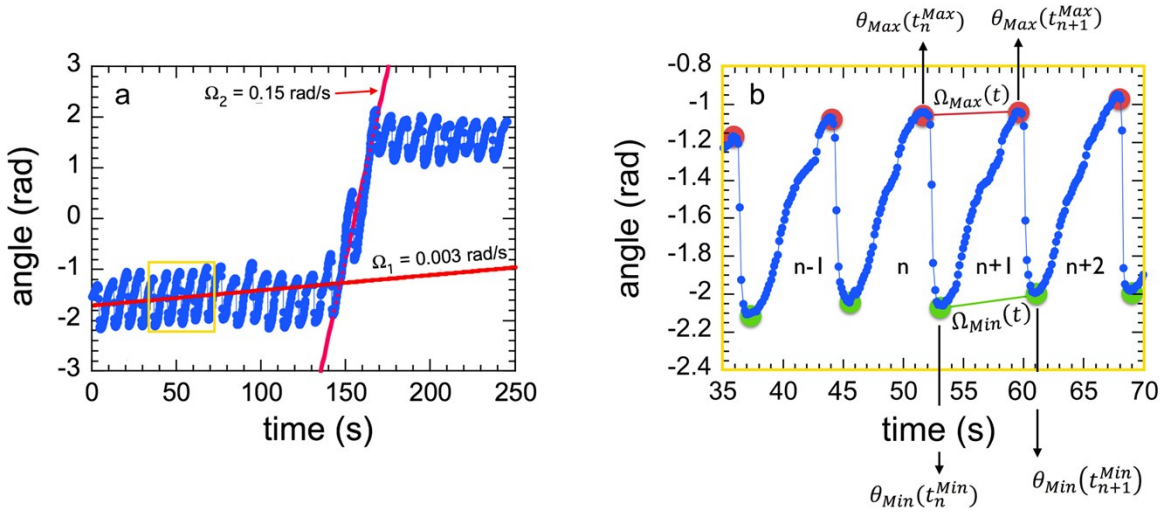

Figure S4: **a)** Orientation angle as a function of the time for a 2.8 µm wire actuated at the frequency ω = 0.36 rad s^{-1}. The straight lines in red are linear regression approximations in selected time ranges. **b)** Close-up view of the data in a) between 35 and 70 s. The definitions of the different maximum and minimum angles (Eqs. S5-1&3), as well as the average times (Eqs. S5-2&4) are provided.

A Matlab plugin was designed to find automatically the $\theta(t)$-minima and maxima for each oscillation, leading to two sets of data, $\Omega_{Max}(t)$ and $\Omega_{Min}(t)$. $\Omega_{Max}(t)$ is defined as:

$$\Omega_{Max}(t_{Max}) = \frac{\theta_{Max}(t_{n+1}^{Max}) - \theta_{Max}(t_n^{Max})}{t_{n+1}^{Max} - t_n^{Max}} \qquad (S4-1)$$

at the time t_{Max} comprised between two successive maxima.

$$t_{Max} = \frac{1}{2}(t_{n+1}^{Max} + t_{n}^{Max}) \qquad (S4-2)$$

The angles $\theta_{Max}(t_{n}^{Max})$ and $\theta_{Max}(t_{n+1}^{Max})$ are indicated in Fig. S4. Similarly, one has

$$\Omega_{Min}(t_{Min}) = \frac{\theta_{Min}(t_{n+1}^{Min}) - \theta_{Min}(t_{n}^{Min})}{t_{n+1}^{Min} - t_{n}^{Min}} \qquad (S4-3)$$

$$t_{Min} = \frac{1}{2}(t_{n+1}^{Min} + t_{n}^{Min}) \qquad (S4-4)$$

where again the angles of interest $\theta_{Min}(t_{n+1}^{Min})$ and $\theta_{Min}(t_{n}^{Min})$ are indicated in Fig. S4. The two quantities $\Omega_{Max}(t)$ and $\Omega_{Min}(t)$ are concatenated and sorted, defining finally the average rotation frequency $\Omega(t)$ as a function of the time. Following this analysis, the number of data points retrieved is twice the number of recorded oscillations.

Two limitations must be considered for the final $\Omega(t)$-data series.

1. There is an intrinsic error in the determination of the wire angle. This uncertainty is linked to the tracking software, as well as in the location of the maximum and minimum angles. In one of our previous studies, it was shown that this uncertainty varies with the wire length (Figure 3 in ref. [1]) and that for a 3 µm wire, this error is 10^{-2} rad. In the experiment shown, this corresponds to an error on $\Omega(t)$ of 2×10^{-3} rad s^{-1}. This analysis has been carried out at each frequency and results in the removal of the so-called outliers. These outliers correspond very high viscosity and represent less than 5% of all data in a given series.
2. Also removed were the $\Omega_{Max}(t)$ and $\Omega_{Min}(t)$ values which were found negative in the previous equations. Negative rotation frequencies were also attributed to errors generated to the tracking software.

Once the outliers removed, the time series are detrended and the data are made equid

Supplementary Information S5 – Parameters derived from the Generalized Random Walk and Ornstein-Ühlenbeck Process (OUP) models

---

In Table S5 are summarized the parameters that can be obtained from the GRW and OUP models.

Statistical function	**Model**	Eq.	τ_l	T_l	α	σ^2	A_T
Auto-correlation function $C(l)$	e^{-t/τ_l}		X				
	Double of Lag at first min			X			
Variogram $\gamma(l)$	Double of Lag at first max			X			
	GRW- Lag 1-2	8			X	X	
	OUP- Lag 1-2	9	X			X	
	GRW – Lag 1-7	6			X	X	
	OUP – Lag 1-7	7	X			X	
	GRW-HE	11		X	X	X	X
	OUP-HE	11	X	X		X	X

Table S5: List of the models and equations used and of the parameters that can be derived from fitting ACF and variogram functions. τ_l, T_l, α, σ^2 and A_T are respectively the correlation time, the period of the oscillations (both in lag units), the coefficient characterizing the autoregressive behavior, the variance and the amplitude of the Hole effect. For the OUP-HE model, the first term in Eq. 11 should be replaced by Eq. 7.

Supplementary Information S6 – Analysis of shear elastic modulus fluctuations obtained by means of optical tweezers in HELA cells (PhD thesis from Ming-Tzo Wei, Lehigh University, 2014)

Recent micro-rheology work by means of optical tweezers in HELA cells [2] shows a time series of the elastic modulus, G', showing large fluctuation for the most rigid substrate, in contrast to the data obtained on the less rigid substrate [3]. The data are reproduced in Fig. S6-1.

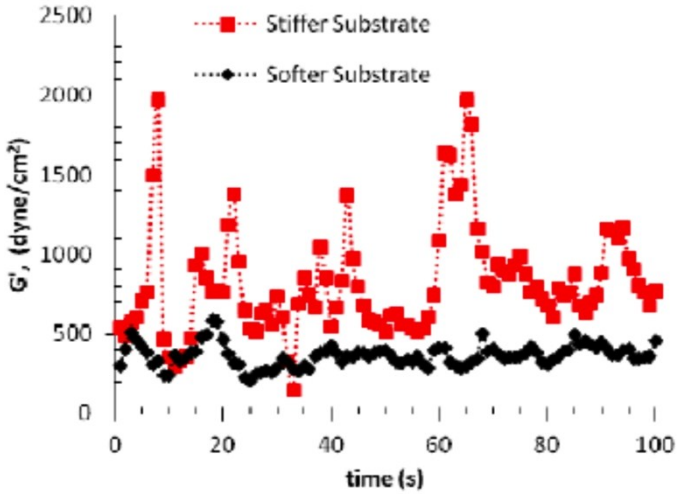

Figure S6-1: Fluctuations of intracellular elastic modulus at 1 Hz as a function of time for Hela cells obtained from optical tweezers measurements using a soft (0.35 kPa) and a stiff (20 kmPa) poly(acrylamide) substrates (from Ming-Tzo Wei, PhD thesis, Lehigh University, 2014) [3].

The data of the most rigid substrate were digitalized and subsequently evaluated in the same way as the micro-rheological data in the present work.

In Fig. S6-2a, 2b and 2c are shown the raw $G'(\omega)$-data (units of Pa), the data without the outliers and the data after making them equidistant, respectively. The sequences of treatment and fitting were applied to the $G'(\omega)$-data. Fig. S6-2d, 2e and 2f are displaying the auto-correlation function (ACF) of the elastic modulus time series, the variogram and the experimental cumulative distribution function (CDF) respectively. The variogram was fitted using the Generalized Random Walk model (Eq. 6, continuous line in blue) and by the GRW model modified by a periodic function (Eq. 11, continuous line in red). For the CDF, the Cauchy (green line), Gauss (blue line) and t-Student distributions are shown for comparison (dashed red and black line to be compared with the red and black dots, being the negative and positive G' changes).

As a result, sub-diffusive, autoregressive, behavior (α = 0.56) and a periodic feature of 23 s have been found in both the ACF and variogram. The variance obtained from our wire based active rheology analysis compares well with the figures obtained from the $G'(\omega)$-data. It is here remarkable that the elasticity fluctuations reveal the same signature

as for the intracellular viscosity. In the Wei *et al.* paper [2], the larger fluctuations of the intracellular elasticity were ascribed to myosin activity, coupled to the rigidity of the substrate. The time scale reported for the lamellipodia contractions of 20 - 30 s falls in the right time range. More work would be necessary to explore and confirm the possible relation between these observations.

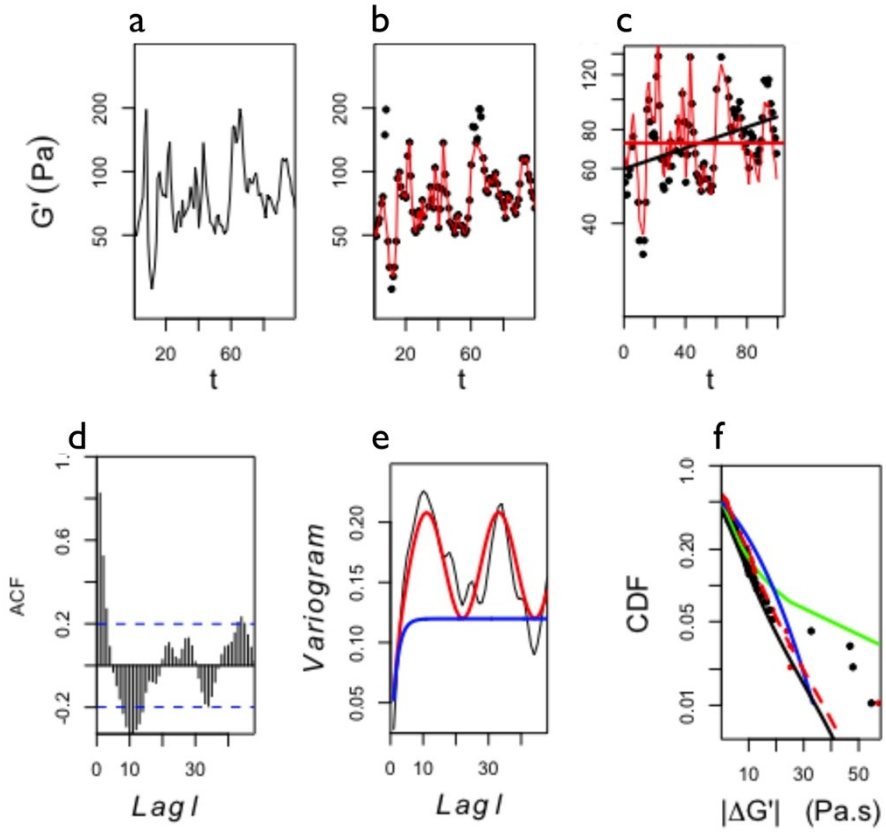

Fig S6-2: Full data analysis cycle showing the main results (digitizing the elastic moduli from the living cells cultured on a polyacrylamide substrate with an elastic modulus of 20 kPa, from M.T. Wei, PhD thesis, Lehigh University (2014) [3]. Starting data **(a)** after outliers removal **(b)**, detrending and making equidistant points **(c)**. The ACF **(d)** and experimental variogram **(e)** are shown as a function of the lag, together with the adjustment using Eq. 11 (GRW-HE model), providing a period T = 23 s and the values for α = 0.56 and σ^2 = 0.041. The experimental cumulative distribution function (CDF) of the modulus **(f)** is well accounted for by the t-Student distribution.

Supplementary Information S7 – Adjustment of the cumulative distribution function (cdf) with Gaussian fits

---

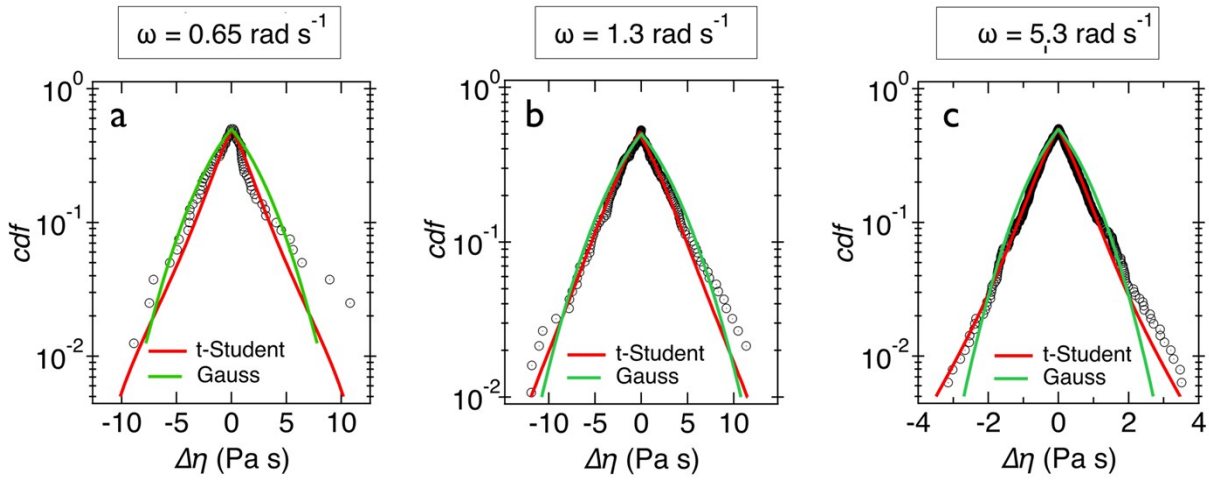

Figure S7: Experimental cumulative distribution function (cdf) of the viscosity variations $\Delta\eta$ at ω = 0.65, 1.3 and 5.3 rad s^{-1}. The Gaussian distributions are shown for comparison. The fittings are complementary of those shown in Fig. 5 in the main text.

Supplementary Information S8 – Frequency dependent autocorrelation time $\tau(\omega)$ obtained from different models and from 3 different wires

---

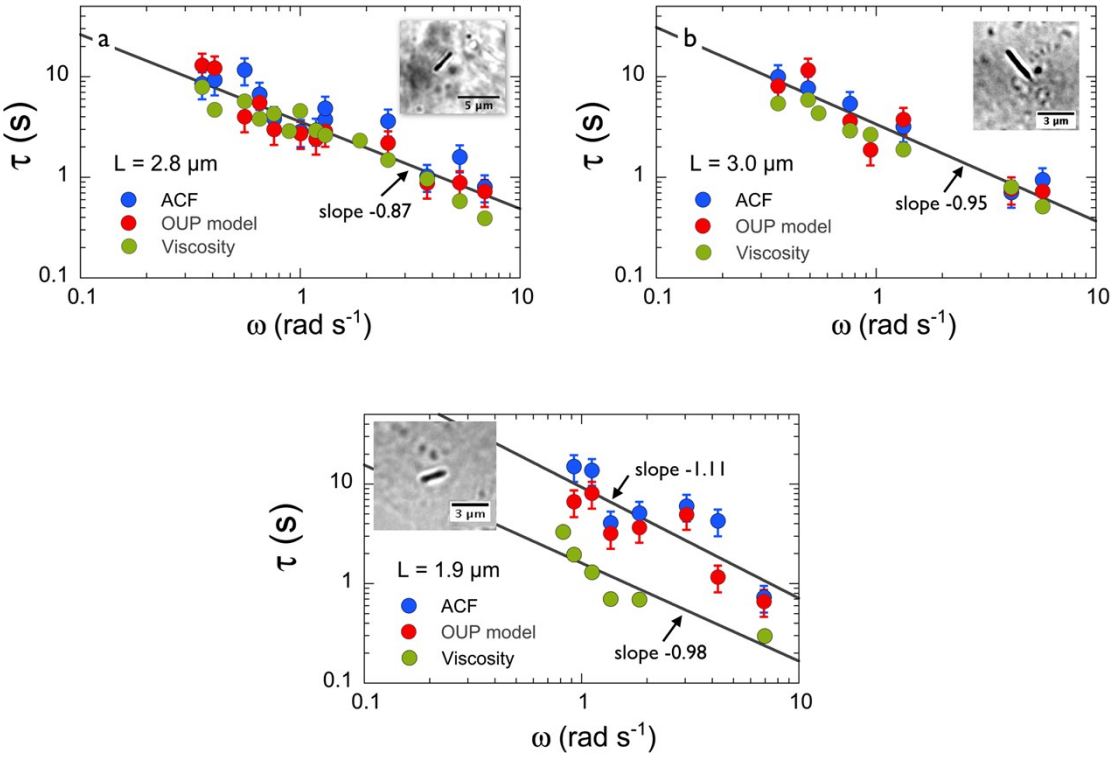

Figure S8: Frequency dependence of the relaxation time $\tau(\omega)$ derived from the ACF (blue circles) and variogram (red circles) functions for L = 2.8 µm **(a)**, L = 3.0 µm **(b)** and L = 1.9 µm **(c)**. The variogram was analyzed using the OUP model (Eq. 7). Also plotted are the ratios $\eta(\omega)/G_0$, where the $\eta(\omega)$ denotes the viscosity displayed in Fig. 4 and G_0 the elastic modulus derived from independent measurements [4]. The insets show the wires in the fibroblast cells. The straight are from least square calculations using a power law of the form: $\tau(\omega) \sim \omega^{\delta}$. The δ-values are indicated.

Supplementary Information S9 – Values of the parameters obtained by fitting data series obtained on three different wires

Method	Eq.	T (s)	α	σ^2	A_T
ACF		100 ± 37	--	--	--
GRW (Lag 1-2)	8	--	0.60 ± 0.15	0.11 ± 0.044	--
GRW (Lag 1-7)	6	--	0.72 ± 0.15	0.12 ± 0.047	--
GRW-HE	11	124 ± 39	0.57 ± 0.17	0.10 ± 0.045	0.18 ± 0.14
OUP (Lag 1-2)	9	--	--	0.20 ± 0.10	--
OUP (Lag 1-7)	7	--	--	0.16 ± 0.055	--
OUP-HE	11	120 ± 35	--	0.19 ± 0.10	--

Table S9-1: Values of the parameters T, α, σ^2 and A_T retrieved from fitting ACF and variogram functions with the GRW, GRW-HE, OUP and OUP-HE models. Values are averaged over 14 frequencies between 0.1 and 7 rad s^{-1}. The data are for a wire of length 2.8 μm

Method	Eq.	T (s)	α	σ^2	A_T
ACF		128 ± 46			
GRW (Lag 1-2)	8		0.71 ± 0.15	0.094 ± 0.001	
GRW (Lag 1-7)	6		0.43 ± 0.05	0.090 ± 0.001	
GRW-HE	11	133 ± 53	0.46 ± 0.18	0.087 ± 0.032	0.19 ± 0.15
OUP (Lag 1-2)	9			0.110 ± 0.002	
OUP (Lag 1-7)	7			0.166 ± 0.006	
OUP-HE	11	132 ± 54		0.149 ± 0.004	

Table S9-2: Same as in Table S9-1 for a 3.0 μm wire. The values are averaged over 8 frequencies between 0.1 and 5 rad s^{-1}.

Method	Eq.	T (s)	α	σ^2	A_T
ACF		148 ± 38			
GRW (Lag 1-2)	8		0.32 ± 0.16	0.10 ± 0.01	
GRW (Lag 1-7)	6		0.64 ± 0.04	0.10 ± 0.01	
GRW-HE	11	146 ± 60	0.68 ± 0.07	0.10 ± 0.01	0.25 ± 0.06
OUP (Lag 1-2)	9			0.12 ± 0.02	
OUP (Lag 1-7)	7			0.16 ± 0.03	
OUP-HE	11	141 ± 49		0.16 ± 0.02	

Table S9-3: Same as in Table S9-1 for a 1.9 μm wire. The values are averaged over 8 frequencies between 0.1 and 7 rad s^{-1}.

References

[1] R. Colin, et al., *Soft Matter*, 10 (**2014**) 1167-1173.
[2] M.-T. Wei, et al., Optical-Tweezers-Based Microrheology of Soft Materials and Living Cells, in: A.H.-P. Ho, D. Kim, M.G. Somekh (Eds.) Handbook of Photonics for Biomedical Engineering, Springer Netherlands, Dordrecht, **2017**, pp. 731-753.
[3] M.T. Wei, Micro-rheology of soft matter and living cells in equilibrium and non-equilibrium systems, Lehigh University, Bethlehem (USA), 2014.
[4] J.-F. Berret, *Nature Communications*, 7 (**2016**) 10134.